

PAPER • OPEN ACCESS

MEMS displacement generator for atomic force microscopy metrology




To cite this article: M Babij *et al* 2021 *Meas. Sci. Technol.* **32** 065903

View the [article online](#) for updates and enhancements.

You may also like

- [Direct writing of three-dimensional Cu-based thermal flow sensors using femtosecond laser-induced reduction of CuO nanoparticles](#)
S Arakane, M Mizoshiri, J Sakurai et al.
- [Superconducting protector against electromagnetic pulses based on YBCO film prepared on an Al₂O₃ substrate with a CeO₂ sublayer](#)
V Vertelis, T Stankevic, S Balevicius et al.
- [\(Digital Presentation\) Epitaxially Grown of SiGe on Ge Microbridge and Observation of Strong Resonant Light Emission](#)
Takahiro Inoue, Youya Wagatsuma, Reo Ikegaya et al.

MEMS displacement generator for atomic force microscopy metrology

M Babij¹, W Majstrzyk¹, A Sierakowski², P Janus² , P Grabiec², Z Ramotowski³, A Yacoot⁴  and T Gotszalk¹ 

¹ Wrocław University of Science and Technology, ul. Z. Janiszewskiego 11/17, PL-50372 Wrocław, Poland

² Łukasiewicz Research Network - Institute of Electron Technology, Al. Lotników 32/46, PL-02668 Warszawa, Poland

³ Central Office of Measure, ul. Elektoralna 2, 00-139 Warsaw, Poland

⁴ National Physical Laboratory, Hampton Road, Teddington, Middlesex TW11 0LW, United Kingdom

E-mail: teodor.gotszalk@pwr.edu.pl

Received 31 July 2020, revised 13 October 2020

Accepted for publication 19 October 2020

Published 6 April 2021



CrossMark

Abstract

Atomic force microscopy enables three-dimensional high-resolution imaging of surfaces with nanoscale features. In order to obtain the quantitative information about surface geometry, the atomic force microscope's scanning system must be calibrated. This is usually done by using calibration samples of known and/or defined shape based on either lithographic or crystal structures. In this work we report on a microelectromechanical device, referred to as a displacement generator, whose vertical deflection is controlled electronically. The designed, fabricated and applied device is formed out of a silicon nitride doubly clamped lever, referred to as a microbridge, with a deposited pair of platinum strips. When the MEMS displacement generator is immersed in a magnetic field and when it is electrically biased, the associated Lorentz force induces a structural displacement. In the presented design, the silicon nitride microbridges were fabricated on a (110) silicon wafer in a Wheatstone bridge configuration. A second reference cantilever was mechanically supported by the silicon substrate. In this way, a highly symmetrical structure was fabricated, making it possible to control precisely deflection in Z direction with sub-nanometre precision. The cantilever's high resonance frequency, of ca. 500 kHz, makes the constructed device insensitive to external vibration sources which are typically at much lower frequencies. As the stage function can be described using the simple harmonic oscillator model, it is clear that the system can operate with sub-nanometre resolution, which, for the purpose of microscope calibration, is extremely beneficial. By placing of the atomic force microscope tip on the actuated reference device it is possible to determine the response of the system over a wide frequency bandwidth. In this work we will describe the fabrication process of the MEMS displacement generator, interferometric and traceable investigations of thermomechanical and electromagnetic actuation schemes. Moreover, we will present the results of the calibration of an atomic force microscope operating in contact and intermittent contact modes.

Keywords: nanometrology, scanning probe microscopy, MEMS

(Some figures may appear in colour only in the online journal)



Original content from this work may be used under the terms of the [Creative Commons Attribution 4.0 licence](https://creativecommons.org/licenses/by/4.0/). Any further distribution of this work must maintain attribution to the author(s) and the title of the work, journal citation and DOI.

1. Introduction

Calibration of the scan and topography axes of scanning probe microscopes is essential not just for turning these microscopes from qualitative imaging tools into quantitative tools that can be used for metrology but also for giving greater confidence in the instrument's performance and the integrity of results obtained using them [1]. Dimensional calibrations are usually realised via calibration standards; two dimensional gratings for the lateral scan axes and step height standards for the vertical axes. These standards would typically be calibrated using metrological atomic force microscopes developed by national metrology laboratories [2]. Metrological atomic force microscopes usually have separate scanning stages for the sample and the cantilever tip together with optical interferometers to measure the relative displacement of the sample with respect to the cantilever. Traceability for length measurements, *i.e.* relating them to the definition of the metre with a known uncertainty, comes via the laser wavelength and the displacement measured in terms of optical fringes. For calibrating the Z or topography axis of a non-metrological atomic force microscope, a step height standard is used and the height of the step determined using either a histogram fit of the data or fit according to the ISO5436 standard [3]. It is necessary to calibrate the whole of the topography axis as any part of it could be used during the scan and there could be both long-range and short-range errors in the motion of the atomic force microscope. The current range of step height standards suffice for the long range, however, for shorter ranges, less than 8 nm, there is a lack of available step height standards. In recent years there have been several approaches to address this problem. An obvious solution is to turn to nature and to use atomic standards based on crystal lattices. Some early work by NIST [4–6] demonstrated this concept with silicon substrates that had staircases of atomic steps. However, processing of data was complicated because the ISO step height fitting routine could not be used and the step widths were narrow (less than 10 μm). Nevertheless, the idea of using silicon was highly appropriate since the lattice parameter of silicon has been measured for the Avogadro project [7] and is quoted in the International Science Council's Committee on Data (CODATA) [8] list of physical constants. The idea of using a symmetric step of silicon was demonstrated [9] leading to the European Metrology Research Programme project CRYSTAL [10] in which the idea of using amphitheatre like structures with large plateaus of atomically flat regions overcame was developed. In 2019 the use of these atomic steps for the calibration of scanning probe microscopes was formally recognised in the *Mise en Pratique* for the metre [11, 12] and further work has been undertaken on the processing of measurements of these steps [13]. An alternative approach that has been considered is the development of active calibration samples where a displacement is generated to perturb the microscope tip by a known distance. This can be achieved using a calibrated piezo electric actuator [14]. Another method applied to fabricate reference structures, is the technology of micro-electromechanical systems (MEMS)

technology. MEMS devices are machines of micrometre size, whose deflection of the movable parts is sensed and controlled electrically. MEMS devices are therefore of high interest for metrology, because of their small dimensions implying small activation energy needed for their operation. Moreover, their high resonance frequency makes the structure insensitive to many environmental disturbances of mechanical and thermal nature. MEMS technology is also very flexible, resulting in relatively simple integration of the MEMS structures with advanced measurement instrumentation. In this way an electrostatic MEMS device was designed for nanorobotics applications to apply the force at the probe in two directions with nanonewton resolution [15]. The electrostatic MEMS devices were also developed to calibrate the lateral force response of an atomic force microscope [16–18]. In this case such a device was placed under the microscope cantilever and by biasing the structure, the lateral reference twist of the probe was induced. Piezoresistive cantilever structures were also applied as a portable force standard and again the idea was to mount the piezoresistive microbeam in place of the sample [19]. The limitation of the electrostatic technology, despite the traceability of the capacitance metrology, is the fact that in order to induce micrometer deflections the structures must be biased with relatively high voltages (~ 40 V per micrometre) which, due to the associated high electric field, can when used in air, attract the dust particles blocking the structure movement. Moreover, the electrostatic actuators cannot be applied in liquid environment, although in vacuum applications they seem to be very efficient. The electromagnetic MEMS offer more flexibility. By careful engineering of the structure elasticity it is possible to apply force and induce structural deflection with high precision. A noticeable solution was proposed by Tian *et al* [20]. In this setup, a macroscopic electromagnetic actuator coupled with a capacitive sensor was applied to induce a calibrated force acting at the atomic force microscope cantilever's tip. In our paper we report on a MEMS microbridge made out of a silicon nitride thin film with a metallization line. When the electrically biased microbridge is immersed in a magnetic field and permanently fixed in a yoke, which acts also as the structure holder, the described device can be used as a deflection generator for an atomic force microscope. The advantage of the proposed technology is that the structure deflection is controlled by the electromagnetic force, which can be controlled with high resolution. As the consequence the structure deflection can be generated over a range of several nanometres in the wide frequency bandwidth from DC up to frequencies less than structure resonance frequency (usually of hundreds of kilohertz). The designed and fabricated deflection generator was used to test the response of an atomic force microscope operating in contact and intermittent modes. The MEMS deflection generator's performance was measured with a reference optical interferometer illuminated with a helium neon (HeNe) laser and then used to calibrate the atomic force microscopes. The investigations were conducted for various interactions forces exerted by the microtip acting on the deflection generator.

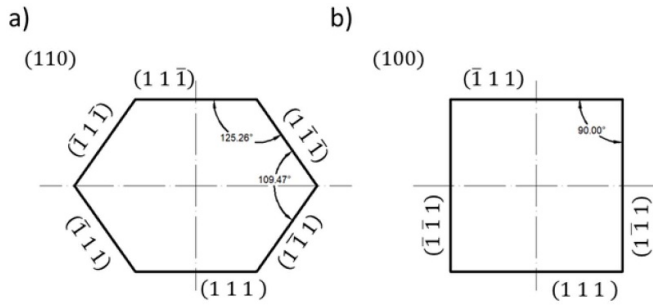


Figure 1. Angles between planes $\{111\}$ at the level of intersection with the wafer surface for two different wafer crystallographic orientation: (a) (110); (b) (100).

2. Material and methods

2.1. MEMS microbridge fabrication

The MEMS displacement generator presented in this paper is a double clamped beam with an integrated electromagnetic deflection actuator. The manufacturing process is based on a technological sequence described in [21, 22]. Depending on the application this technology allows to apply various metals forming the conductive paths. For simple reflective layers thin, 10 nm Al can be deposited in the last step. For the resistive suspended structures require Cr/Pt layers which can withstand Si etching in alkaline solutions. In brief, in the first step a silicon nitride layer (500 ± 1 nm thick) was deposited onto a silicon wafer using low pressure vapour deposition. In the second step 20 ± 1 nm chromium (as an adhesion layer) and 200 ± 1 nm platinum layers were deposited onto the silicon nitride using a sputtering technique in order to form the metallization layer. Next, using dry plasma etching of the platinum and the silicon nitride, the metallization paths and shapes of microbridges were formed. Finally, structures were released by wet silicon etching in potassium hydroxide (KOH) solution.

In this way, the double clamped beam was formed as a composition of silicon nitride and platinum/chromium layers. In contrast to our previous technology, in which as a substrate a (100) wafer was applied as a substrate [4], we used a (110) silicon wafer as a supporting base of the MEMS displacement generator.

The geometry of the structure defined on the mask is shown in figure 2(a). However, prior to the experiments dimensions of each structure were verified using a high resolution optical microscope.

On a (110) wafer, a group of six equivalent planes belonging to $\{111\}$ family intersect the surface of the wafer. This plane configuration is different from the plane configuration on a (100) silicon wafer where only a group of four equivalent $\{111\}$ planes intersect the surface of the silicon substrate. As the result the angles between planes $\{111\}$ at the plane of intersection with the surface of the (110) wafer are 120° compared to 90° in the case of a (100) wafer as shown in figure 1.

The use of (110) wafers is advantageous as the intersecting $\{111\}$ planes are not perpendicular to each other. In this case it is possible to fabricate a microbridge, whose long axis is perfectly perpendicular to the edges of the silicon beam supporting area as shown in figure 2.

As the result, the microbridge can be positioned on a (110) substrate perpendicular to the crystal directions $[\bar{1}10]$ between edges A and B-figure 2.

Figures 3(a) and (b) present scanning electron microscope images of the microbridge structures fabricated on (110) and (100) wafers respectively. The (110) microbridge is uniformly strained, whereas the (100) microstructure at the beam supporting points is not symmetrically underpinned, which affects the uniformity of the structure displacement needed for the reliable atomic force microscope calibration.

2.2. Electromagnetic actuation

The deflection of the MEMS deflection generator is controlled electromagnetically. When the microbridge is immersed in the magnetic field \vec{B} and biased by the current \vec{I}_b the electromagnetic force \vec{F}_{el} can be calculated according to the formula [22]:

$$\vec{F}_{el} = (\vec{I}_b \times \vec{B}) l \quad (1)$$

where l is the effective length of the conductive loop segment perpendicular to the magnetic field lines. When the magnetic field is uniform and directed perpendicularly to the microbridge long axis, the electromagnetic force: $F_{el} = I_b B l$ is vertical with respect to the microbridge structure causing the vertical structure deflection. These conditions are achieved with great precision as the strong neodymium permanent magnets used to supply the magnetic field are much bigger than the MEMS microbridge resulting in a homogenous magnetic field around the structure. Moreover, the deflection generator is securely mounted in a yoke, which ensures the repeatability of the measurements performed with various instrumentation and the bias current can be controlled electronically in the wide bandwidth with high resolution. The electromagnetic force F_{el} causes maximal structure deflection y_{max} in the middle of the microbridge according to the equation: $y_{max} = \frac{F_{el} l^3}{384 E I}$, where E is the effective Young modulus of the microbridge, I is the microbridge inertia moment. The effective Young modulus and inertia moment are difficult to calculate for the microstructures comprising multi material layers whose intrinsic mechanical stresses are different and unknown. Therefore the microbridge was characterized experimentally and described by the stiffness determined as the ratio of the applied electromagnetic force and the induced structure displacement: $k = \frac{F_{el}}{y_{max}}$.

2.3. Measurement setup

A SIOS SP120 optical vibrometer illuminated with a stabilized He-Ne laser was used to calibrate the vibration amplitude of the MEMS displacement generator. The resolution of

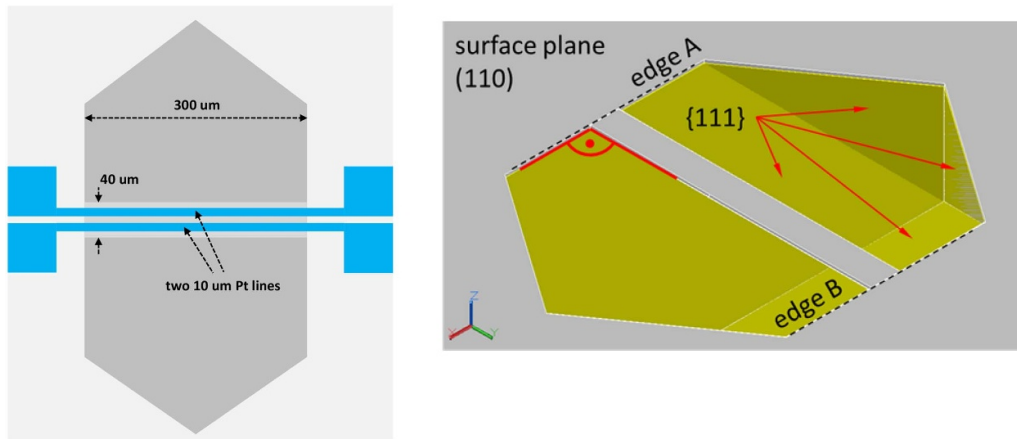


Figure 2. (a) Geometry of the deflection generator structure (b) proper mask design for silicon nitride rectangular microbridges fabrication on a (110) silicon wafer. Edges A and B marked on the figure overlap with the crystal direction $[\bar{1}10]$.

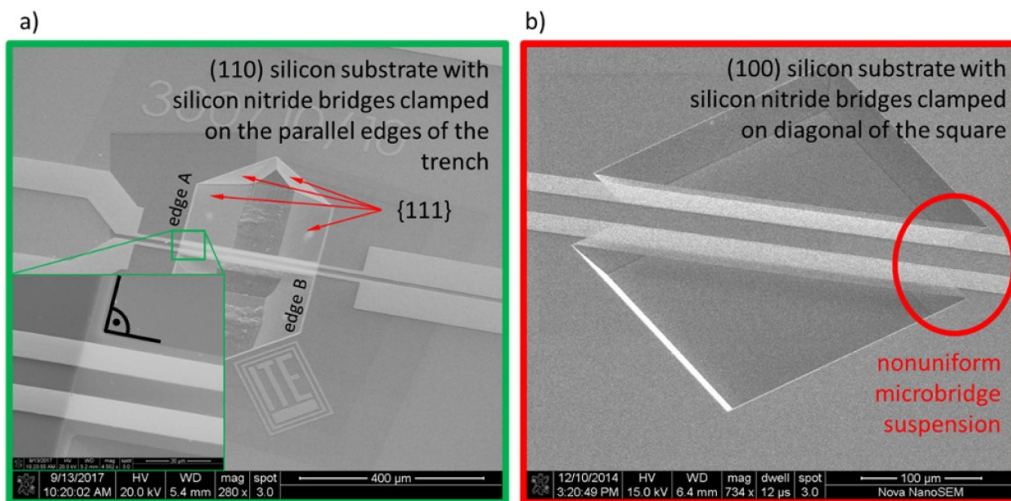


Figure 3. Double clamped silicon nitride bridges as a MEMS displacement generator with platinum metallization paths: (a) fabricated on a (110) silicon substrate, (b) fabricated on a (100) silicon substrate.

the vibrometer was, according to the manufacturer's specification, 5 pm. Atomic force microscopy (AFM) experiments and vibrometer measurements were performed at room temperature in ambient conditions. The bridge was actuated electromagnetically in a custom-made yoke containing neodymium magnets and acting as the structure holder. The magnetic field of 0.6 T in the middle of the holder, where MEMS bridge was located, was measured using a commercial Teslameter. The current passing through the metallization lines of the bridge was determined with the uncertainty of 0.01% and was supplied by a calibrated Howland source pump (HCS). The HCS was controlled by a Tektronix AFG3021B arbitrary waveforms generator.

AFM calibration experiments were performed in contact and resonance intermittent modes using cantilevers with stiffnesses and resonance frequencies of 0.13 N m^{-1} , 6 kHz and 3.45 N mm^{-1} , 75 kHz respectively. The same displacement generator, mounted permanently in the same magnetic yoke, was investigated using the interferometer and atomic force microscope under calibration. All the AFM measurements

were performed using a NanoMan Veeco Instruments microscope. The NanoScope Analysis 1.5 software was used for data processing [23]. The set-up is shown in figure 4.

3. Results

In first experiments, the MEMS displacement generator was measured using the vibrometer. In this way, as the microbridge resonance frequency, in the range of several hundreds of kHz, was far higher than the low-frequency system disturbance. The small signal operation (SSO) of the MEMS displacement generator can be described using a simple harmonic oscillator (SHO) model. In this case, one can assume that the structure stiffness k is linear. As the consequence, the static reference deflection can be calculated based on the resonance microbridge deflection, which, due to the interferometer's traceability, selective signal acquisition and 5 pm resolution, was measured with the low uncertainty and the best achievable signal to noise ratio

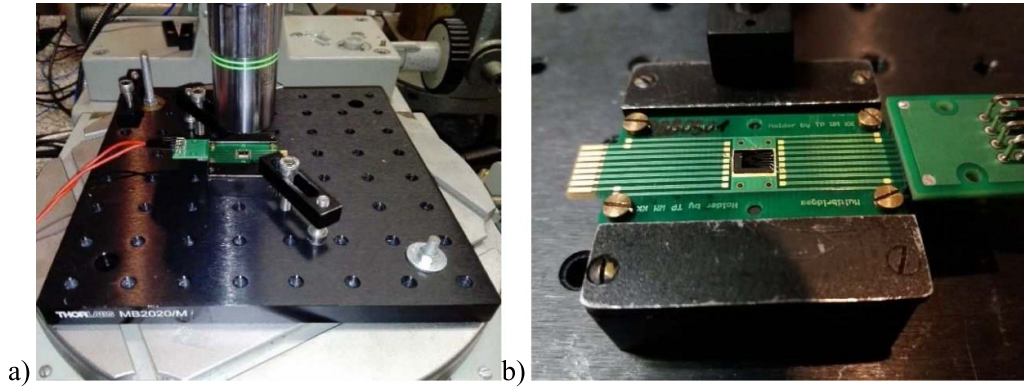


Figure 4. Experimental setup for MEMS displacement generator calibration, (a) general view, (b) closeup on the MEMS structure mounted in magnetic holder.

Table 1. Parameters of microbridge deflection reference-SSO calibration.

| I_b (μA) _{rms} | f_r (Hz) | z_r (nm) _{rms} | Q | F_{el} (nN) _{rms} | k (N m^{-1}) | A (nm mA^{-1}) |
|--|------------|---------------------------|-----|------------------------------|---------------------------|-----------------------------|
| 40 | 511943 | 2.1 | 166 | 4.8 | 412.3 | 0.31 |
| 100 | 511872 | 5.1 | 164 | 12.0 | 414.1 | 0.31 |
| 200 | 511848 | 10.1 | 167 | 24.0 | 393.4 | 0.30 |

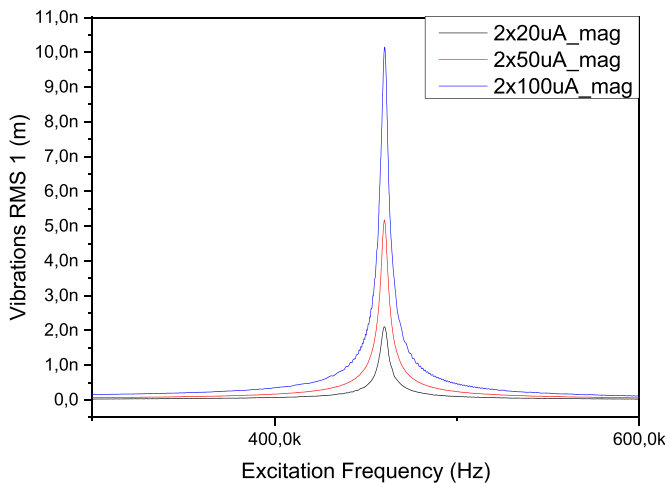


Figure 5. MEMS displacement generator resonance behaviour actuated by the electromagnetic force.

(SNR). The resonance microbridge vibration was measured for 40, 100 and 200 μA_{rms} bias currents I_b (see figure 5). Table 1 summarizes the measured resonance frequency f_r , resonance structure deflection z_r , determined structure quality factor Q , calculated electromagnetic force $F_{el} = I_b l$ and deflection generator stiffness: $k = \frac{F_{el} Q}{z_r}$.

As the position of the magnetic field source under the microbridge reference is fixed it is useful, from a general point of view, to calculate the structure deflection based on the actuation sensitivity: $A = \frac{z_r}{Q I_b}$.

The obtained SSO results: resonance frequencies and quality factors are consistent for the applied bias currents. The calculated differences stem from the precision of the fitting algorithm used for the resonance curve analyses and the

limited resolution of the interferometer used for the measurement of the microbridge vibration, especially for the small microbridge displacement recorded for the bias current of 40 μA .

The results obtained clearly suggest, that in order to actuate the static structure deflection in the range of several nanometres, which is needed for atomic force microscope calibration, bias currents in the range of several mA are necessary. In this case, in the so-called large signal operation (LSO) mode, the SHO calibration procedure cannot be applied as the elasticity of the vibrating in the resonance microbridge becomes nonlinear. When, the microbridge reference was biased with a sinusoidal current of 8 mA_{rms} at frequency of 25 Hz, corresponding to power dissipation in the actuator of 25.6 mW and electromagnetic force of 960 nN, the measured structure deflection was 2.8 nm_{rms} corresponding to 7.9 nm_{pp} . The calculated LSO actuation sensitivity was in this case 0.35 nm mA^{-1} . It is higher than in SSO mode, which results in heating of the microbridge reference. The increased temperature decreases, in this case, the overall structure stiffness, which is a linear function of Young modulus E . Moreover, as the dependence of the Young moduli vs. temperature is linear, the changes of the microbridge reference stiffness depend on the thermal Young modulus sensitivity. The Young moduli of Si_3N_4 and platinum are both around 160 GPa, but the thermal sensitivities differ significantly and are 0.01 GPa K^{-1} and $3.4 \times 10^{-4} \text{GPa K}^{-1}$ respectively [24, 25]. In this case, considering only the changes of the Si_3N_4 properties one can calculate the temperature increase of 10 K, when the microbridge was biased with current of 8 mA_{rms} .

In the AFM experiments, the MEMS microbridge reference integrated with magnets and a yoke was mounted under the atomic force microscope scanning head. The AFM cantilever was aligned parallel to the microbridge as shown in figure 6.

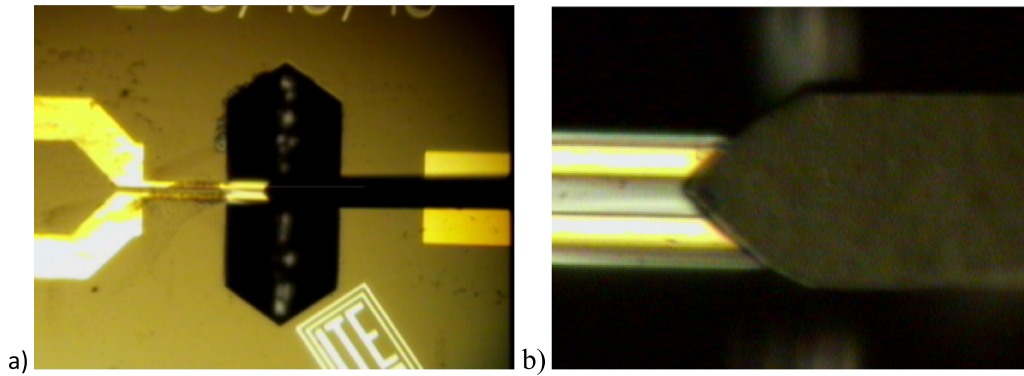


Figure 6. AFM cantilever above the MEMS bridge, (a) general view, (b) close-up on the centre of the displacement generator.

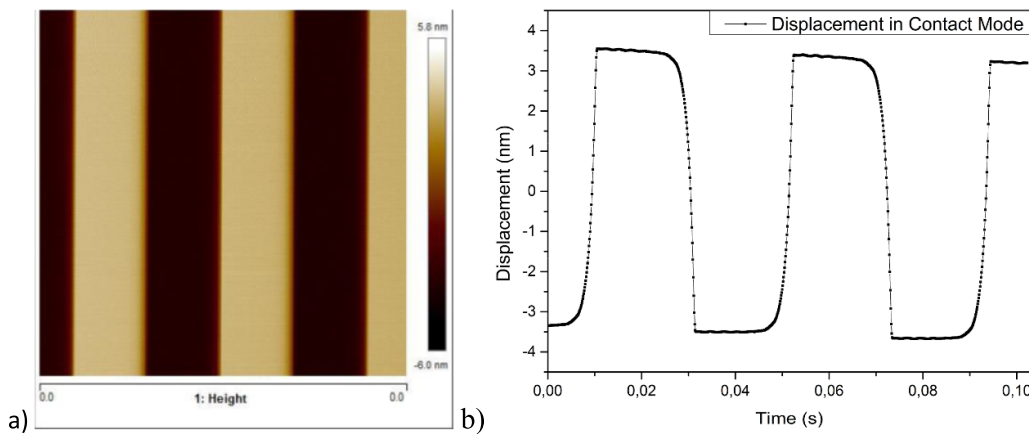


Figure 7. Electromagnetically actuated MEMS displacement generator-deflection amplitude observed with a microscope operating in C AFM mode.

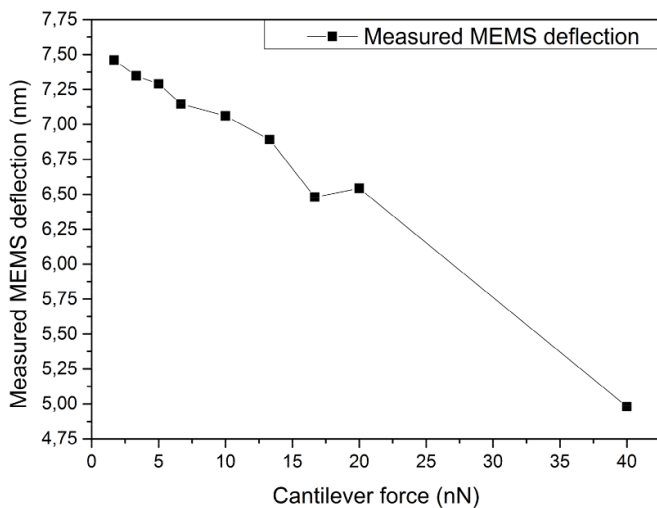


Figure 8. Electromagnetically actuated MEMS displacement generator-measurements performed using a contact atomic force microscope with a range of different load forces.

The tip was brought into contact with the MEMS displacement generator as in standard AFM routines. After the tip approach both metallization lines of the microbridge were biased with a square-waved current of 4 mA amplitude and frequency of 24.4 Hz.

The AFM measurements were conducted when the XY microscope scanner was switched off. The microscope feedback loop was active and compensated for the deflection of the microbridge reference. In this way the cross-sections of the images, which were acquired by performing a scan with no actual displacement of the cantilever in X and Y, corresponded to the changes of the deflection of the MEMS bridge. In every experiment the position of the tip over the deflected microbridge reference was adjusted to find the position at which the structure deflection was maximum. In the first AFM experiments the deflection of the electromagnetic MEMS deflection reference was measured by a contact mode atomic force microscope using a soft cantilever with stiffness of 0.12 N m^{-1} . The PID controller was set to be fast enough to follow the MEMS reference deflection- see figure 7. The amplitude of the recorded AFM image is 7.46 nm_{pp} which corresponds with the amplitude of 7.87 nm_{pp} measured for the same bias current using an interferometer. It should be noticed, however, that the numbers given by the microscope’s software are based on the previous system calibration according to the procedure described by the microscope manufacturer and the difference is within the uncertainty associated with the calibration. The recorded signals reflect the time constant of the PID controller feedback loop of 5 ms, which was much smaller than the time constant of the MEMS reference $\tau = \frac{2Q}{\omega_0} = \frac{Q}{\pi f_r}$

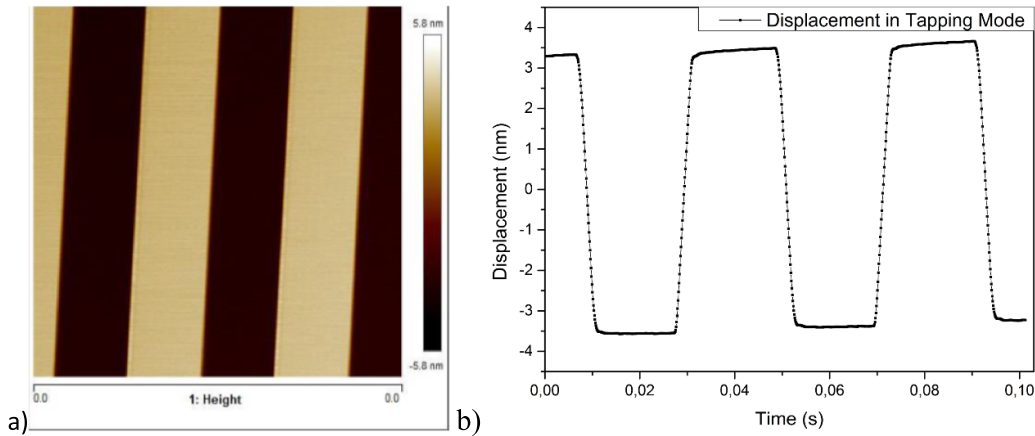


Figure 9. Electromagnetically actuated MEMS displacement generator-deflection amplitude observed using a microscope operating in IM AFM mode.

of ca. 250 μs (resonant frequency ca. 510 kHz, quality factor Q of 130).

The deflection amplitude was measured for a range of forces between 1.7 nN and 40.0 nN applied to the cantilever; results are shown in figure 8. To perform reliable measurements with low error the low force setpoint is crucial, as we expect that the microbridge is strained just under the tip.

The deflection of the electromagnetic MEMS displacement generator was investigated in intermittent contact mode (IM) as well. In these experiments we used a cantilever with a spring constant of 3.4 N m^{-1} and resonance frequency of 225.6 kHz.

In IM AFM mode, the setpoint of the reduction in amplitude of the cantilever's oscillation when the tip is engaged with the surface is chosen such that the image obtained has optimum resolution without the tip causing damage to the surface.

Typically, we scan the surface when the cantilever oscillation is reduced to between 20%–30% of the free beam vibration. The deflection tests using the electromagnetic MEMS deflection generator were carried out therefore for these two setpoints (20% and 30%)

As in contact measurements, the PID controller was set to follow the microbridge displacement generator and the metalization were biased with a current of 8 mA. The results for the 30% setpoint are presented in figure 9.

The amplitude taken from the crosssection of the image, recorded in the same manner as it was measured in C-AFM, is 7.0 nm_{pp} . The difference between the interferometer measurement and the result given by the atomic force microscope, stems from the discrepancy between the position at which the structure deflection was observed and the scaling of the microscope scanner. The height recorded for 20% setpoint did not exhibit any difference from the results measured for 30% setpoint.

The results obtained indicated that the interactions in IM experiments were smaller than in CM AFM measurements. It should be also notified, that the displacement generator was controlled with the same frequency of 3 Hz in IM and CM experiments and the PID controller was tuned in order to obtain a stable system response. In IM experiments, the differential PID component was reduced and the system

responded slower than in CM investigations—see figures 8(b) and 9(b). However, it should be noted that the calibration of an atomic force microscope using the proposed displacement generator was carried out in a manner similar to that used for calibrations using conventional step height standards in accordance to ISO 5436 [3]. In this way, the transition phase, which is shortened as much as possible by proper PID controller tuning, should not be taken into account.

4. Summary

In this paper we presented a MEMS based displacement generator that can be used to generate a known displacement which can in turn be used to evaluate the atomic force microscope performance in the single nanometre range for users outside of a national metrology institute. The new type of MEMS displacement generator was designed, fabricated and characterized. The doubly-clamped beams were etched on (110) wafers orientation to achieve very well defined clamping areas, so the bridges are rectangular in shape. We calibrated the vibrations of the microbridge using commercial laser vibrometer. Measurements were made of the vibration amplitude of the electromagnetically driven MEMS bridge using an atomic force microscope operated in both contact and intermittent contact modes. The experiments showed that to achieve agreement between the vibration amplitude measured with the tested microscope and deflection measured with the laser vibrometer the calibration should be performed with the atomic force microscope operated in contact mode using a cantilever with relatively low stiffness. It is accepted that further work is required to produce a complete uncertainty budget for the performance of the MEMS displacement generator in order to establish the full traceability. However, the work presented in this paper clearly proves the concept and potential of the device. Future studies will consider uncertainty sources in more detail and measure the performance of the device using a metrological AFM. It should be also noted, that the MEMS displacement generator presented in this paper can be used to characterize the microscope performance when the

metallization line would be biased with the so called common voltage, not influencing the bias current but defining the structure potential. In this way additional tests in Kelvin force probe microscopy (KPFM) can be performed making it possible to analyse the resolution possibilities and crosstalk issues.

Acknowledgments

This work was supported by the National Science Center (NCN) PRELUDIUM grant ‘Displacement metrology of nano-electro-mechanical systems (NEMS) based on scanning tunneling microscopy methods’ (Grant Nos. 2016/21/N/ST7/02275).

ORCID iDs

P Janus  <https://orcid.org/0000-0002-6720-5540>
 A Yacoot  <https://orcid.org/0000-0001-6740-821X>
 T Gotszalk  <https://orcid.org/0000-0003-4182-9192>

References

- [1] Danzebrink H U, Koenders L, Wilkening G, Yacoot A and Kunzmann H 2006 Advances in scanning force microscopy for dimensional metrology *CIRP Ann. -Manuf. Technol.* **55** 841–78
- [2] Yacoot A and Koenders L 2011 Recent developments in dimensional nanometrology using AFMs *Meas. Sci. Technol.* **22** 122001
- [3] ISO 5436-1:2000 2000 Geometrical product specifications (GPS) – surface texture: profile method; measurement standards – part 1: material measure
- [4] Tsai V W, Vorburger T, Dixon R, Fu J, Koning R, Silver R and Williams E D 1998 The study of silicon stepped surfaces as atomic force microscope calibration standards with a calibrated AFM at NIST Characterization and metrology for ULSI technology *AIP Conf. Proc.* vol 449 ed D Seiler, A C Diebold, W M Bullis, T J Shaffner, R McDonald and E J Walters pp 839–42
- [5] Fu J, Tsai V, Koning R, Dixon R and Vorburger T 1999 Algorithms for calculating single-atom step heights *Nanotechnology* **10** 428–33
- [6] Dixon R, Orji N, Fu J, Tsai V, Williams E, Kacker R and Nyffenegger R 2001 Silicon single atom steps as AFM height standards *Proc. SPIE* **4344** 157–68
- [7] Andreas B et al 2011 Determination of the Avogadro constant by counting atoms in a ^{28}Si crystal *Phys. Rev. Lett.* **106** 030801
- [8] Mohr P J, Taylor B N and Newell D B 2012 CODATA recommended values of the fundamental physical constants: 2010 *Rev. Mod. Phys.* **84** 1527–605
- [9] Yacoot A, Koenders L and Wolff H 2007 An atomic force microscope for the study of the effects of tip sample interactions on dimensional metrology *Meas. Sci. Technol.* **18** 350–9
- [10] Crystalline and self-assembled structures as length standards (www.ptb.de/emrp/sib61-home.html)
- [11] Consultative Committee for Length 2019 Mise en Pratique for the definition of the metre in the SI (<https://www.bipm.org/utis/en/pdf/si-mep/SI-App2-metre.pdf>)
- [12] Consultative Committee for Length 2019 Recommendations of CCL/WG-N on: realization of SI metre using height of monoatomic steps of crystalline silicon surfaces (<https://www.bipm.org/utis/common/pdf/CC/CCL/CCL-GD-MeP-3.pdf>)
- [13] Garnes J, Necas D, Nielsen L, Madsen M H, Torras-Rossel A, Zeng G, Klapetek P and Yacoot A 2020 Algorithms for using silicon steps for scanning probe microscope evaluation *Metrologia* **57** 1–14
- [14] Koops R, van Veghel M and van de Nes A 2016 A virtual lateral standard for AFM calibration *Microelectron. Eng.* **153** 29–36
- [15] Beyeler F, Muntwyler S, Nagy Z, Graetzel C, Moser M and Nelson B J 2008 Design and calibration of a MEMS sensor for measuring the force and torque acting on a magnetic microrobot *J. Micromech. Microeng.* **18** 2
- [16] Cumpson P J and Hedley J 2003 Accurate analytical measurements in the atomic force microscope: a microfabricated spring constant standard potentially traceable to the SI *Nanotechnology* **14** 1279–88
- [17] Cumpson P J, Hedley J and Zhdan P 2003 Accurate force measurement in the atomic force microscope: a microfabricated array of reference springs for easy cantilever calibration *Nanotechnology* **14** 918–24
- [18] Cumpson P J, Hedley J and Clifford C A 2005 Microelectromechanical device for lateral force calibration in the atomic force microscope: lateral electrical nanobalance *J. Vac. Sci. Technol. B* **23** 1992–7
- [19] Ingo B, Lutz D and Erwin P 2003 Piezoresistive cantilever as portable micro force calibration standard *J. Micromech. Microeng.* **13** S171
- [20] Tian Y, Zhou C, Wang F, Zhang J, Guo Z and Zhang D 2018 A novel method and system for calibrating the spring constant of atomic force microscope cantilever based on electromagnetic actuation *Rev. Sci. Instrum.* **89** 125119
- [21] Moczala M, Kopiec D, Sierakowski A, Dobrowolski R, Grabiec P and Gotszalk T 2014 Investigations of mechanical properties of microfabricated resonators using atomic force microscopy related techniques *Microelectron. Eng.* **119** 164–8
- [22] Moczala M, Babij M, Majstrzyk W, Sierakowski A, Dobrowolski R and Janus P 2016 Sensors and Actuators A : physical technology of thermally driven and magnetotively detected MEMS microbridges *Sensors Actuators A* **240** 17–22
- [23] Świądkowski B, Piasecki T, Rudek M, Świątkowski M, Gajewski K, Majstrzyk W, Babij M, Dzierka A and Gotszalk T 2020 ARMScope – the versatile platform for scanning probe microscopy systems *Metrologia Meas. Syst.* **27** 119–30
- [24] Farraro R and McLellan R B 1977 Temperature dependence of the Young’s modulus and shear modulus of pure nickel platinum, and molybdenum *Metall. Trans. A* **8** 1563–5
- [25] Bruls R J, Hintzen H T, De With G and Metselaar R 2001 The temperature dependence of the Young’s modulus of MgSiN₂, AlN and Si₃N₄ *J. Eur. Ceram. Soc.* **21** 263–8